Science of the Total Environment 563–564 (2016) 386–395

Contents lists available at ScienceDirect

Science of the Total Environment

journal homepage: www.elsevier.com/locate/scitotenv

Using geochemical indicators to distinguish high biogeochemical activity in floodplain soils and sediments

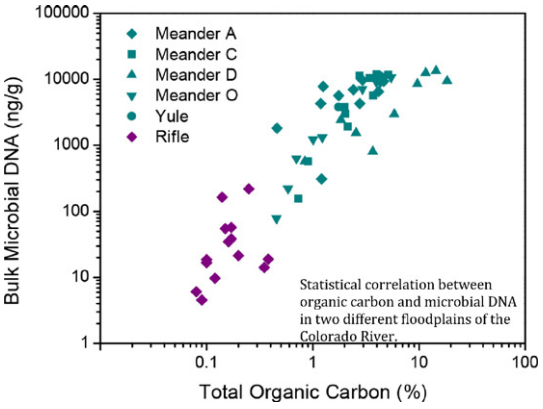
Amy Kenwell [a], Alexis Navarre-Sitchler [a,*], Rodrigo Prugue [a], John R. Spear [b], Amanda S. Hering [c], Reed M. Maxwell [a], Rosemary W.H. Carroll [d], Kenneth H. Williams [e]

[a] Hydrologic Sciences and Engineering Program, Colorado School of Mines, 1500 Illinois St., Golden, CO 80401, United States
[b] Department of Civil and Environmental Engineering, Colorado School of Mines, 1500 Illinois St., Golden, CO 80401, United States
[c] Department of Applied Mathematics and Statistics, Colorado School of Mines, 1500 Illinois St., Golden, CO 80401, United States
[d] Desert Research Institute, Division of Hydrologic Sciences, 2215 Raggio Parkway, Reno, NV 89512, United States
[e] Lawrence Berkeley National Laboratory, Berkeley, CA 94720, United States

HIGHLIGHTS

- Biogeochemical characterization of alluvial floodplain soils and sediments was performed to investigate parameters that may indicate microbial hot spot formation.
- A correlation between geochemical parameters (total organic carbon and extractable metals) and bulk microbial DNA was found in two alluvial floodplain settings.
- Results of this study motivate additional work on understanding the influence of environment on microbial activity, and microbial activity on environment in natural systems.

GRAPHICAL ABSTRACT



ARTICLE INFO

Article history:
Received 25 January 2016
Received in revised form 2 April 2016
Accepted 3 April 2016
Available online 1 May 2016

Editor: Jay Gan

Keywords:
Microbial DNA
Extractable metals
Floodplain geochemistry

ABSTRACT

A better understanding of how microbial communities interact with their surroundings in physically and chemically heterogeneous subsurface environments will lead to improved quantification of biogeochemical reactions and associated nutrient cycling. This study develops a methodology to predict potential elevated rates of biogeochemical activity (microbial "hotspots") in subsurface environments by correlating microbial DNA and aspects of the community structure with the spatial distribution of geochemical indicators in subsurface sediments. Multiple linear regression models of simulated precipitation leachate, HCl and hydroxylamine extractable iron and manganese, total organic carbon (TOC), and microbial community structure were used to identify sample characteristics indicative of biogeochemical hotspots within fluvially-derived aquifer sediments and overlying soils. The method has been applied to (a) alluvial materials collected at a former uranium mill site near Rifle, Colorado and (b) relatively undisturbed floodplain deposits (soils and sediments) collected along the East River near Crested Butte, Colorado. At Rifle, 16 alluvial samples were taken from 8 sediment cores, and at the East River, 46 soil/sediment samples were collected across and perpendicular to 3 active meanders and an oxbow meander. Regression models using TOC and TOC combined with extractable iron and manganese results were determined to be

* Corresponding author.
E-mail address: asitchle@mines.edu (A. Navarre-Sitchler).

http://dx.doi.org/10.1016/j.scitotenv.2016.04.014
0048-9697/© 2016 Elsevier B.V. All rights reserved.

the best fitting statistical models of microbial DNA (via 16S rRNA gene analysis). Fitting these models to observations in both contaminated and natural floodplain deposits, and their associated alluvial aquifers, demonstrates the broad applicability of the geochemical indicator based approach.

© 2016 Elsevier B.V. All rights reserved.

1. Introduction

Heterogeneous distributions of chemical and physical parameters in the subsurface exert control on important hydrologic, geochemical and microbial processes, but connectivity between these systems is poorly understood (Chen and MacQuarrie, 2004; Hedin et al., 1998; Boano et al., 2014). Variations in organic matter, nitrogen, iron and other metals can be found in natural systems at scales down to a centimeter and smaller (Schilling and Jacobson, 2012; Englert et al., 2009; Murphy et al., 1997; Boano et al., 2014). These variations contribute to microbial activity in the subsurface through availability of terminal electron acceptors and electron donors required for microbial metabolism (Sena et al., 2012; García-Balboa et al., 2011; Hakala et al., 2009). Thus, prediction of the distribution of microbial activity may be possible by defining geochemical indicators of biogeochemical activity. If such an approach is valid, simple geochemical tests can enhance our ability to identify important areas for detailed microbial characterization in natural systems. Of particular interest are operationally defined biogeochemical hotspots or small-scale heterogeneities where microbial activity is high relative to the bulk or average microbial activity of the larger system. Biogeochemical hotspot formation may be driven by high organic carbon and high bioavailable metal concentrations (Hakala et al., 2009).

Heterogeneous distributions of microbial populations can result from variations of moisture content and geochemical conditions (Pinay et al., 2007; Schilling and Jacobson, 2012; Murphy et al., 1997), especially dissolved oxygen. Spatial separation of microbial communities, driven by available terminal electron acceptors can be very strong in lakes and aquifers (Sweerts et al., 1991; Chapelle and Lovley, 1992) but tends to be less distinct in fluvial systems due to substantial groundwater-surface water mixing that induces fluctuations in redox conditions (Morrice et al., 2000). In hyporheic zones, aerobic surface water mixes with groundwater (Boano et al., 2014) generating strong gradients in chemical conditions that stimulate microbial communities and drive much of the microbial activity in fluvial systems (Prommer et al., 2006; Hill et al., 2000; Hedin et al., 1998; McDowell et al., 1992).

Field observations of relationships between physical and chemical heterogeneity and microbial activity in subsurface materials are limited (Hedin et al., 1998; Pinay et al., 2000; Campbell et al., 2012), but are needed in order to parameterize and constrain conceptual and numerical models (Fleckenstein et al., 2010; Boano et al., 2014; Englert et al., 2009). This study evaluated the empirical relationships between geochemical properties of subsurface materials and bulk microbial DNA in soil and sediment samples from a stranded floodplain in Rifle, Colorado and an active floodplain on the East River, Colorado with linear statistical models. The objective of the study was to explore whether such models can provide a basis for (1) targeting areas for detailed analysis of microbial activity and structure and (2) simplification of numerical simulation of biogeochemical processes in this system. The two flood plains are sites of extensive and active research in subsurface microbial activity and represent different depositional processes and morphology so that statistical relationships across two sites can be compared.

Heterogeneous distributions of redox conditions and microbial populations are challenging aspects of subsurface modeling (Atchley et al., 2013; Li et al., 2011; Boano et al., 2014; Beisman et al., 2015). Co-dependence between distributions of geochemical properties of soils and development of microbial community structure would simplify model parameterization (Englert et al., 2009; Sena et al., 2012; Murphy et al., 1997; Prommer et al., 2006). If empirical relationships can be consistently identified between subsurface properties and microbial properties, microbial characteristics may be predictable based on only chemical and physical analyses.

1.1. Site descriptions

Two study sites that are the focus of extensive research on subsurface biogeochemical activity and microbial populations were chosen for this study.

1.2. Rifle, Colorado

The U.S. Department of Energy (DOE) field biogeochemistry study site in Rifle, Colorado is a stranded floodplain on the banks of the Colorado River (Fig. 1). The site consists of Wasatch Formation bedrock overlain by Quaternary alluvium sediment. Uranium contaminated alluvial sediments were removed in 1996 during reclamation efforts after closure of a uranium and vanadium mill (DOE, 1999), and the site was capped with ~1.5 m of silt-rich sediment. The Quaternary alluvium sediment consists of fluvial silts, sands and gravels and has a thickness of approximately 6–7.6 m. The Wasatch Formation bedrock is comprised of variegated claystone, siltstone and sandstone lenses that serve as a local aquitard (DOE, 1999). A majority of the water in the alluvial aquifer discharges into the Colorado River, which forms the southern boundary of the field site. More detailed reports on the geology, hydrologic conditions and geochemistry of the site are available (DOE, 1999, 2011; DOE(2), 2011.

1.3. East River, Gothic, Colorado

The East River floodplain is downstream of the Rocky Mountain Biological Laboratory (RMBL) in Gothic, CO (Fig. 1). This watershed exhibits characteristic fluvial progression and serves as a representative example of many headwater catchments within the upper Colorado River basin. The East River valley in the study area is comprised of Mancos Shale bedrock overlain by glacial moraine deposits. Four meanders from the study site with different characteristics were chosen for sampling to maximize the distribution of organic carbon concentrations (Fig. 1). Meander A has a narrow neck and short vegetation with no surface water channels. Meander C is a much longer meander with many potential hyporheic flowpaths and some inner channels and trees. Meander D is large, but contains dry areas with trees as well as regions that are seasonally saturated with wetlands and internal streams. Meander O is a cutoff oxbow meander whose riverbed is seasonally inundated with groundwater and does not contribute substantially to the main flow of the river.

2. Methods

2.1. Sample collection and preparation

2.1.1. Rifle

Samples of alluvial material from the Rifle site were collected from sediment cores extracted during the drilling of wells along the outer edge of the Rifle site in April 2013 (Fig. 2). A total of 16 samples from 8 wells were analyzed. Ten of these samples were collected during

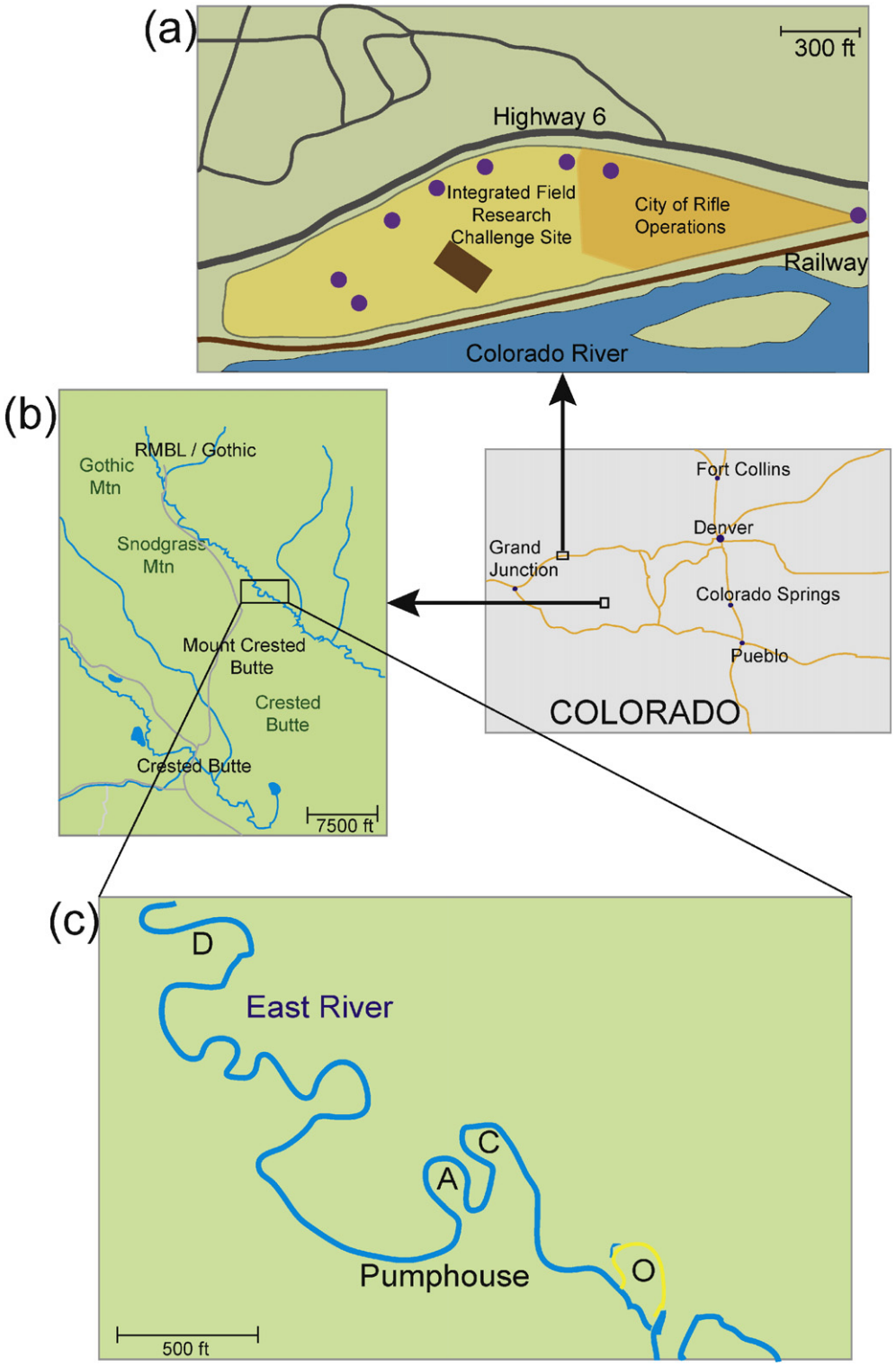


Fig. 1. Location map of (a) Rifle and (b) East River field sites and (c) locations of specific East River meanders A, C, D and O. Location of previous Rifle biostimulation experiments is also indicated by brown rectangle in (a) (Yabusaki et al., 2011).

drilling, transported in 50 ml centrifuge tubes at 4 °C to Colorado School of Mines and frozen. Six samples were collected in June 2014 from the core material archived at the Rifle site at −80 °C.

2.1.2. East River

Soil and sediment samples were collected from four East River meanders (A, C, D and O) (Fig. 2). Samples were collected across the neck and down the body of each meander (Fig. 2). 'Across samples' were distributed along the necks of meanders where hyporheic throughflow could be expected. They were spaced approximately evenly with one sample station at each bank and three inside the meander. 'Down samples' were evenly spaced beginning at the toe of the meander and progressing down the meander axis. The first letter of each sample name (A, C, D or O) refers to which meander the sample was collected from (Fig. 2). The second letter refers to its position, with samples "a" through "e" across the neck of the meander, where "a" is on the

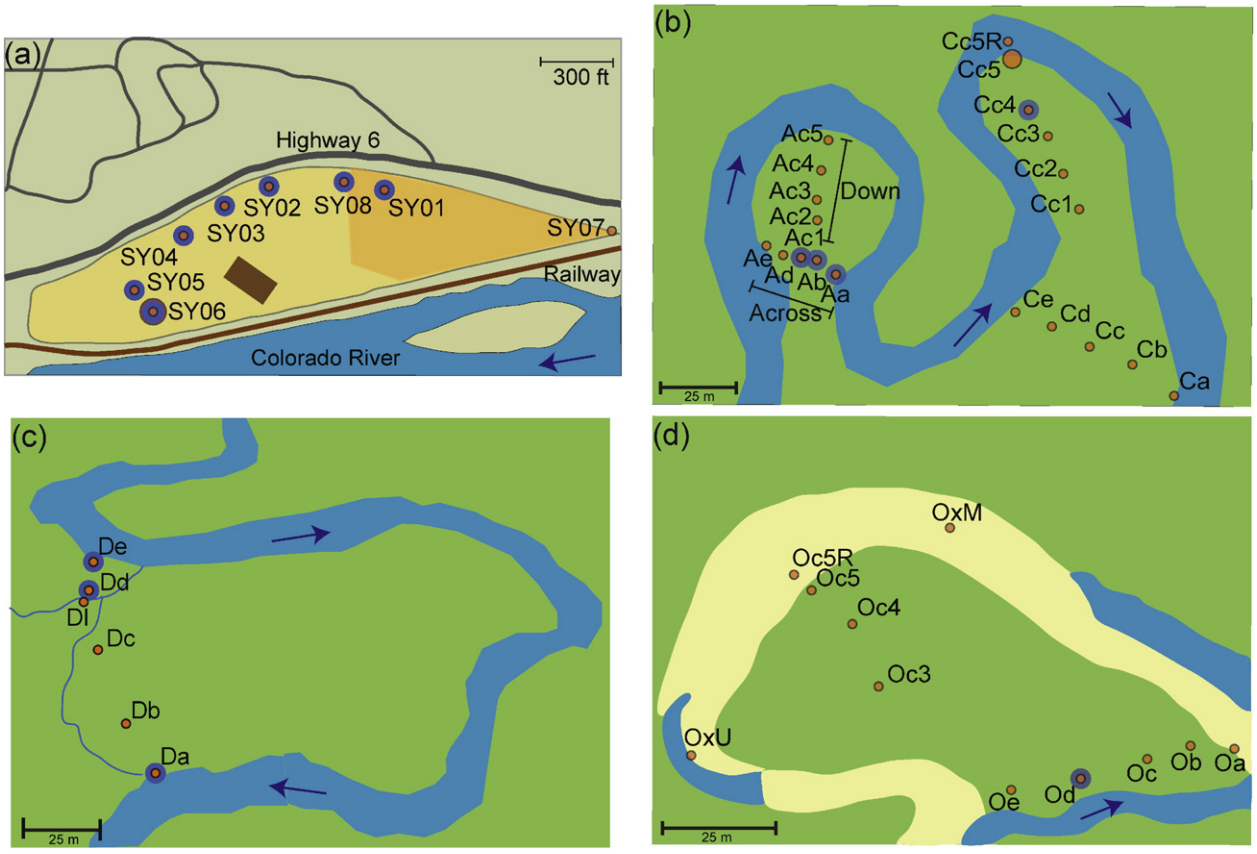


Fig. 2. Sample locations in (a) Rifle Colorado and on meanders (b) A and C, (c) D and (d) O at the East River site. Deeper samples are indicated by purple circles. Flow directions of the rivers are indicated by arrows.

downstream side. Samples collected down the meander axis toward the toe of the meander are labelled "c1" through "c5", with "c5" being nearest the toe. The sample effort constituted 46 soil and sediment samples in total. A grab sample from the riverbed (Cc5R) and an oxidized iron rich sample from a waterway running across the inside of meander D (Dl) were also taken. In the oxbow meander (O), three samples were collected from the cutoff riverbed: one in a stagnant pool (OxU), one at the toe of the down transect (Oc5R) and one in an outcrop of Mancos shale (OxM). An additional sample (Yule) was collected at the Rocky Mountain Biological Lab (RMBL) approximately 5000 m upstream of the sampled meanders.

Surface vegetation was removed using a shovel, and a 16 cm hole was augered. A grab sample was collected beneath the hole using a shovel. Where possible, a second sample was collected 16 cm beneath the first (Cc4D, DaD, DdD and DeD). Samples OdT and OdB refer to stations at the top and bottom of the river bank, respectively. For three sample stations (Aa, Ab and Ac) a hand-corer was used to extract 20–50 cm of soil core. From core Aa, subsamples were taken from the top and bottom of the core. For Ab and Ac, a single core sample was analyzed along with a grab sample.

2.2. Sample preparation and analysis

Collected samples were transported on dry ice to the Colorado School of Mines where they were stored at −20 °C until analysis. Most samples were thawed in an anaerobic chamber (Coy Lab Products, Inc., Grass Lake, MI), and subsamples were collected in sterile 50 ml centrifuge tubes and stored in the anaerobic chamber for chemical extractions. Core samples were not thawed in an anaerobic chamber because the cores were too large for the chamber. However, subsamples from these cores were transferred to the anaerobic chamber soon after thawing to minimize exposure to oxygen. East River subsamples of approximately 5 g (wet mass) were freeze-dried using a FreeZone 6 Liter Benchtop Freeze Dry System (Labconco, Kansas City, MO). Remaining sample material was oven dried at 75 °C and ground to 60 μm for TOC and leach test analyses. Total organic carbon (TOC) analysis was performed on duplicate samples using a CM 5014 Coulometer (UIC, Joliet, IL, USA).

2.3. Iron and manganese extractions

HCl-extractable iron and manganese were recovered by combining 3 g of wet sediment with 150 ml of 0.5 N HCl in an HDPE bottle in an anaerobic chamber. In another bottle, 150 ml of 0.25 N hydroxylamine hydrochloride in 0.5 N HCl was combined with the same amount of wet sediment. Bottles were shaken at room temperature for 24 h ± 15 min, and then fluid was sampled, filtered to 0.45 μm, and acidified with trace metal grade nitric acid. Iron and manganese concentrations in the extractant were determined with ICP-AES. Extractable iron and manganese was reported as the average between these two extraction procedures.

2.4. Synthetic precipitation leaching

Synthetic precipitation leach tests were conducted on East River samples to determine metal mobility in these near-surface samples. This method was adapted from EPA method 1312 for solid phase non-volatile extractions in wastewater (EPA, 1994). The synthetic

precipitation consisted of 60:40 H_2SO_4:HNO_3 in Milliq water adjusted to a pH of 4.2 ± 0.05 to simulate metals released as rainwater leaches through soil. This extraction fluid was combined with dry sediment passed through a 0.991 cm sieve in a 20:1 ratio of extractant to sediment and shaken for 18 h. The extract was sampled, filtered to 0.45 μm, and acidified with trace metal grade for analysis by ICP-AES.

2.5. DNA extraction and quantitative PCR analysis

DNA was extracted from sediment samples using the PowerSoil DNA Isolation Kit (MO BIO Laboratories, Inc., Carlsbad, CA, USA). Extractions were performed according to the manufacturer's directions except that a 1 min bead beating replaced the 10 min vortexing step (Pepe-Ranney et al., 2012). Extracted DNA was stored at −20 °C. Quantitative PCR was performed in triplicate on a Roche LightCycler 480 system (Roche Diagnostics, Indianapolis, IN, USA). Working curves for sediment and groundwater DNA were created by amplifying environmental samples with PCR primers, combining the triplicates and bead purifying them with an Agencourt AMPure XP (Beckman Coulter, Indianapolis, IN, USA). These were quantified using a Qubit 2.0 Fluorometer and Qubit dsDNA High Sensitivity Assay Kit (Life Technologies, Grand Island, NY, USA). Bulk microbial DNA in raw samples was determined using the same system. The results of the Qubit analyses were converted to gene copies using the URI Genomics and Sequencing Center converter (Staroscik, 2004). Quality assurance was performed by analyzing some amplicons via agarose gel electrophoresis and ethidium bromide staining. Negative and positive controls were also analyzed.

2.5.1. 16S rRNA gene PCR primers

Universal primers (for Bacteria, Archaea and Eucarya) were used to amplify 16S rRNA genes (18S for Eucarya) to normalize bacterial gene abundances to obtained functional gene abundances (below). Each well in the 96 well optical plate contained 2 μl of sample DNA, 12.5 μl of PerfeCTa SYBR Green Super Mix (Promega Corporation, Madison, WI, USA), 1 μl each of forward primer EUB338F (5′ACTCCTACGGGAGGCAGCAG) and reverse primer EUB518R (5′ATTACCGCGGCTGCTGG) and 8.5 μl of nuclease-free water. The PCR reactions were run on the LightCycler with pre-incubation at 95 °C for 15 min followed by a PCR protocol of 40 cycles at 95 °C for 60 s, 53 °C for 30 s and 72 °C for 60 s. This was followed by a melting curve protocol of 95 °C for 5 s, 65 °C for 60 s and a continuous drop from 98 °C with final cooling at 40 °C for 10 s (Fierer et al., 2005).

2.5.2. nirK and nirS primers

Conditions in hyporheic zones are particularly favorable for denitrification (Morrice et al., 2000; Hedin et al., 1998), therefore denitrifying *nirK* genes were amplified as above except with primers *nirK*876F (5′ ATYGGCGGVCAYGGCGA) and *nirK*1040R (5′GCCTCGATCAGRTTRTGGTT) while *nirS* genes were amplified with primers *nirS*cd3aF (5′ GTSAACGTSAAGGARACSGG) and *nirS*3cdR (5′GASTTCGGRTGSGTCTTGA). Samples were denatured at 95 °C for 5 min prior to a 6 cycle touchdown at 95 °C for 15 s, 63 °C for 30 s and 72 °C for 30 s. The PCR amplification was 15 s at 95 °C, 30 s at 58 °C and 30 s at 72 °C for 40 cycles. The melt curve was one cycle of 95 °C for 15 s, 55 °C for 1 s and a continuous drop from 99 °C followed by 40 °C for 1 s (Henry et al., 2004; Throbäck et al., 2004).

2.5.3. dsr primers

The presence of sulfate reducing genes was tested using *dsr* gene primers. Each PCR reaction included 2 μl of sample DNA, 10 μl of PerfeCTa SYBR Green Super Mix, 2 μl each primer and 6 μl of nuclease-free water. The primers applied were *dsr*1F+ (5′ACSCACTGGAAGCACGGCGG) and *dsr*-R (5′GTGGMRCCGTGCAKRTTGG) as in Kondo et al. (2004). The PCR protocol began with an initial denaturation at 95 °C for 10 min followed by 40 cycles of PCR amplification of 95 °C for 30 s, 58 °C for 30 s, 72 °C for 40 s, and a continuous drop from 80 °C. The melting curve protocol was 1 s at 55 °C and a continuous drop from 95 °C. Final cooling took place at 40 °C for 1 s.

Table 1
Explanatory variables included in test models.

Model	Variables included
1	TOC
2	Extractable Fe and Mn
3	Leachable Fe and Mn
4	TOC, extractable Fe and Mn
5	TOC, leachable Fe and Mn
6	TOC, extractable Fe and Mn, leachable Fe and Mn

2.6. Statistical methods

Multiple linear regression (MLR) was applied to subsets of the East River and Rifle data using open-source R software (The R Foundation). MLR predicts a response variable (in this case DNA) based on a linear combination of explanatory variables. Six sets of explanatory variables were tested (Table 1) on standardized data transformed into approximately normal distributions as necessary (TOC, DNA and leachable metals were log-transformed). Residuals of the models were assessed for normality using QQ plots and the Shapiro-Wilks test. As a check for heteroscedasticity of the residuals, the standardized residuals were plotted against the fitted values, and any influential points were identified with leverages, which are the diagonal entries of the MLR hat matrix (Sheather, 2009). The fit of each model was compared using the adjusted R^2 value, which accounts for varying numbers of explanatory variables. Each model was also tested on four subsets of the data: All East River, East River Meanders (no meander bend, riverbed or upstream samples) and each of these subsets combined with Rifle alluvial data.

3. Results and discussion

3.1. Total organic carbon (TOC)

3.1.1. Rifle

Total organic carbon content ranged from 0.0 to 0.4 wt% in the Rifle alluvium (Figs. 3 and 4; Table A1). Samples from wells SY-02, SY-03 and SY-06 had the highest organic carbon content within the alluvium with average well concentrations of 0.21%, 0.18% and 0.30%, respectively. Average TOC at the Rifle site was 0.15%. A key consideration in the low carbon content is that the Rifle site is a stranded floodplain that no longer receives seasonal organic matter and trace metals through overbank deposition (Pinay et al., 2000; Du Laing et al., 2009). In addition, the surface material at the site was removed and replaced with fill, which changed the vegetative environment above the alluvium layer.

3.1.2. East River

Total organic carbon (TOC) percentages in the East River averaged 3.9% with a minimum TOC concentration of 0.5% and maximum of 18% (Figs. 3 and 4; Table A2). With 2.4%, 3.0% and 2.9% average TOC, respectively, meanders A, C and O had similar concentrations of TOC and less than half the average of 7.7% TOC in meander D. Where multiple depths were sampled, TOC was lower in deeper samples except at sample location De on the upstream bank of meander D.

At the East River, high TOC values near the toes of meanders A and C may be attributed to recent overbank deposition of organic rich sediments. For inactive meander O, the lowest organic carbon on the progressively inland transect was closest to the dry riverbed. In addition, meanders A and C had slightly lower organic carbon in the c4 samples (Fig. 4), which is where the slowest hyporheic flow and longest

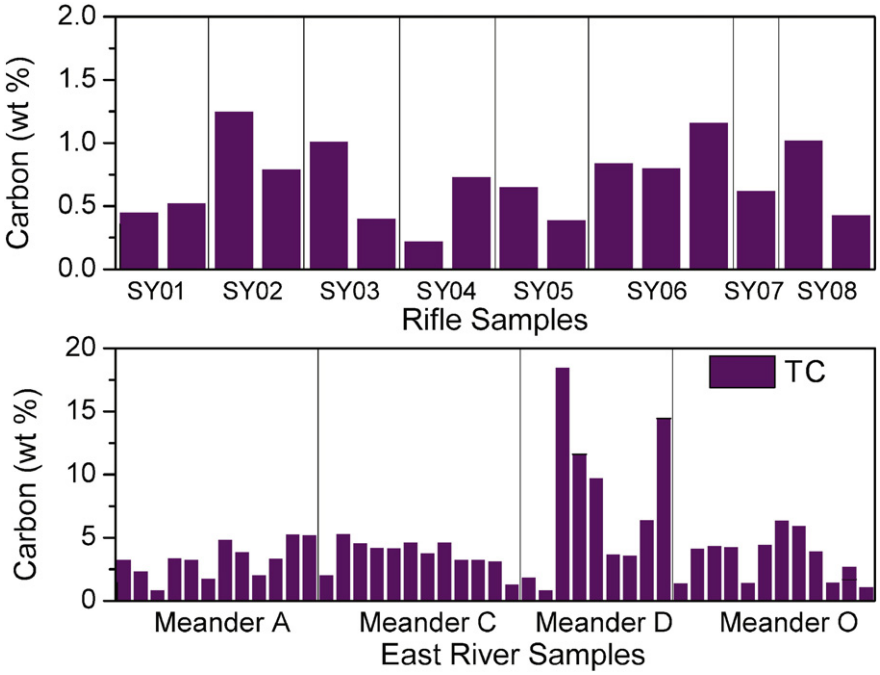


Fig. 3. Total carbon content of alluvial Rifle and East River samples.

flowpaths in the meander are predicted to occur (Revelli et al., 2008). This could reflect increased microbial consumption of organic carbon when the fluid residence time is longer. Meander D is a wide, treed meander, but at the time of sampling, water was running across the neck, so this meander may be in the process of being cut off. The water saturated nature of the sampling area and the predominance of

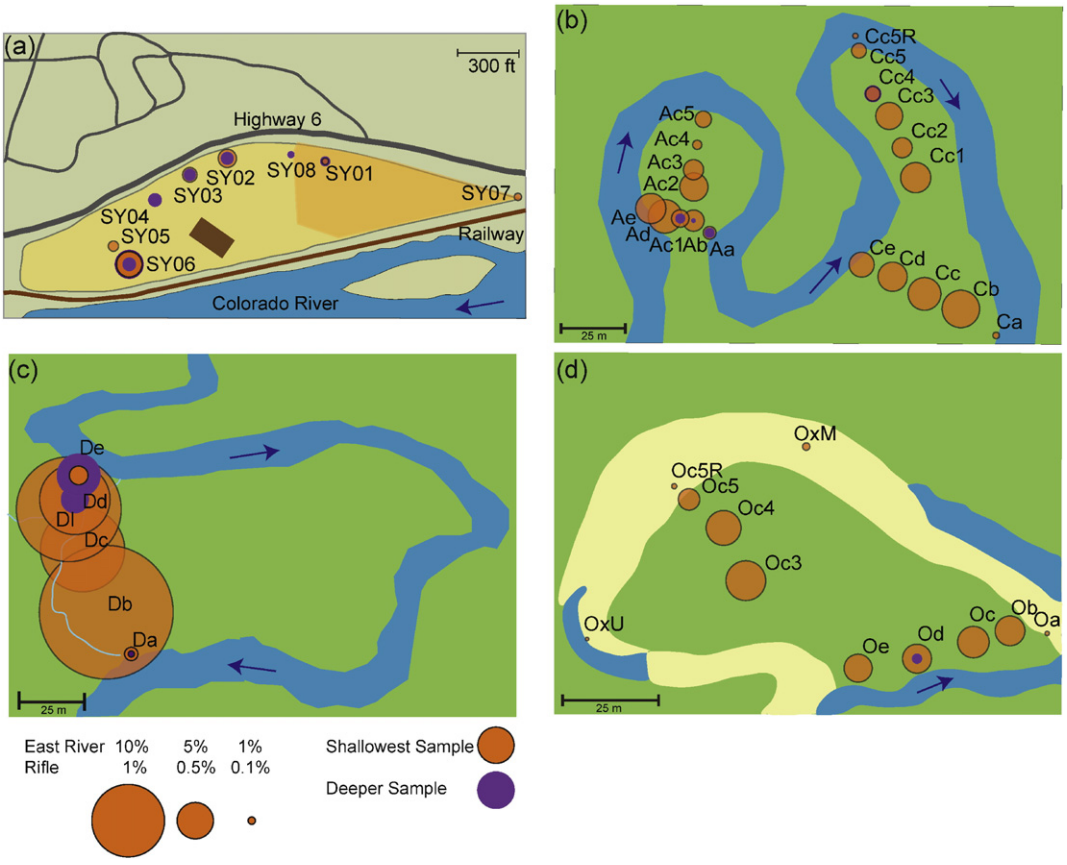


Fig. 4. Distribution of TOC in Rifle (a) and on East River meanders A, C (b), D (c), and O (d) shown with circles. Circle diameter is proportional to TOC percentage with the size of Rifle circles exaggerated 10%. Purple circles indicate deeper samples. High organic content in meander D was likely a result of the wet, marshy neck of this meander.

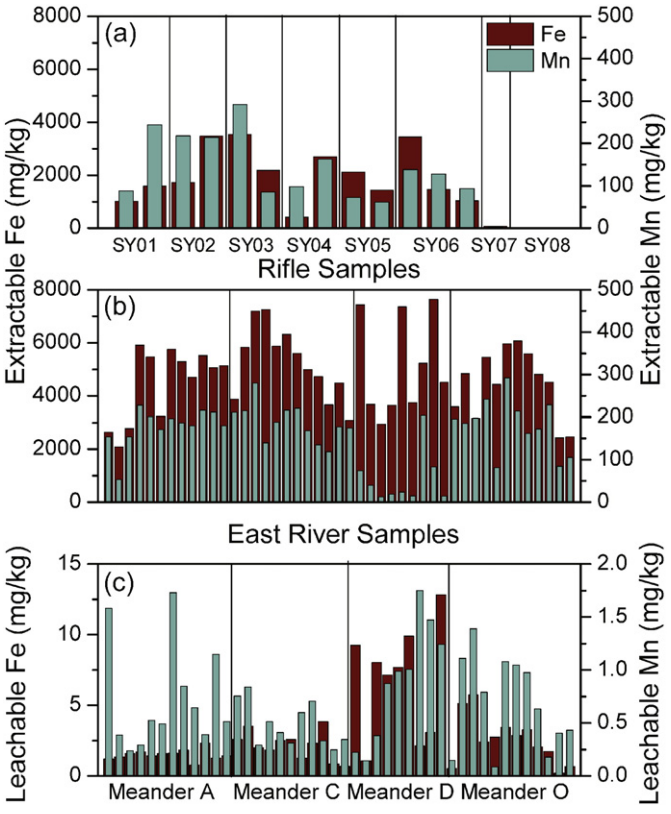


Fig. 5. Average extractable iron and manganese extracted from 0.5 N HCl and 0.25 N hydroxylamine in 0.5 N HCl extractions in (a) Rifle and (b) the East River. (c) Leachable iron and manganese in East River samples from an 18 h test with a pH 4.2 solution of 60:40 sulfuric:nitric acid. Note that leachable metal concentrations are several orders of magnitude lower than extractable metals.

wetland vegetation may explain the very high TOC percentages found in these samples.

3.2. Iron and manganese extractions

3.2.1. Rifle

At the Rifle site, average extractable iron was 1600 mg/kg with a standard deviation of 1200 mg/kg, and average extractable manganese was 120 mg/kg with a standard deviation of 88 mg/kg (Fig. 5). Both metals were quite variable, with iron concentrations between 1 and 3500 mg/kg and manganese between 0 and 290 mg/kg.

3.2.2. East River

For all East River samples, average extractable iron ranged from 900 mg/kg to 7700 mg/kg with an average of 4700 mg/kg and a standard deviation of 1500 mg/kg (Fig. 5). Average concentrations for each meander were similar and ranged from 4400 mg/kg to 5200 mg/kg for meanders A and C, respectively. Concentrations within each meander also exhibited low variability with standard deviations of approximately 1300 mg/kg for meanders A, C and O. The exception was meander D, which had an average extractable iron concentration of 5100 mg/kg and a standard deviation of 1900 mg/kg.

The low extractable metals in the center of meander D may correlate to a high concentration of electron donors (high TOC), which could have led to increased microbial reduction of Fe(III) to Fe(II). This meander also had high water saturation with several moisture contents above 100%, and the mobile Fe(II) could have been transported away by water. In general, samples from locations seasonally inundated by river water (AaT, AaB, Cc5R, OxM and OxU) had lower concentrations of extractable metals than those that remain unsaturated for most of the year.

3.3. Synthetic precipitation leaching

The results from a synthetic precipitation leach test represent metals and metal concentrations that may be easily mobilized during a precipitation event and are therefore readily available for microbial processes. Leach tests were only conducted on samples from the East River site due to the large sample size required for the test and the shallow sampling locations that could be exposed to rainwater infiltration. Leachable iron concentrations varied from 0.17 to 13 mg/kg with an average of 3.1 mg/kg (Fig. 5, Table A7 in supplementary material). Leachable manganese concentrations averaged 0.69 mg/kg with a range from 0.08 mg/kg to 1.8 mg/kg. These concentrations were approximately three orders of magnitude less than HCl-extractable iron and manganese because the simulated precipitation leaching targets only highly mobile metals.

As with extractable metals, meander-specific trends of leachable metals are dependent on small-scale meander environments. For leachable metals, iron was fairly consistent between meanders A, C and O with averages of 1.5 mg/kg, 2.2 mg/kg and 2.7 mg/kg, respectively, while leachable manganese varied between sample locations with a standard deviation of 0.44 mg/kg in comparison with the average of 0.69 mg/kg.

The upstream edge of meander D (Samples De and DeD), as well as the edges of meander A, contained high leachable manganese concentrations. Leachable iron concentrations were generally higher in meander D than all other meanders while leachable manganese had some relatively high concentrations in each meander except meander C. These results suggest that some areas may be manganese reducing, but manganese reduction may not be the dominant reduction reaction on the floodplain. In addition, the high organic carbon and leachable metals in meander D may classify this meander as a potential hotspot of microbial activity worth investigating with additional microbiological techniques. High concentrations of electron donors and terminal electron acceptors make this an ideal habitat where microbial populations can thrive. Meander D may therefore have a disproportionately high influence on the nutrient cycling and geochemistry of the system.

3.4. DNA extraction and quantitative PCR

Here we use bulk microbial DNA (mass) as a proxy for potential or inferred microbial activity in a given sample. This assumption is supported by the strong correlation (for the full dataset an R^2 value of 0.67) between 16S rRNA and bulk microbial DNA and suggests the majority of DNA is representative of bacterial genes. While bulk DNA is only able to provide insight into the potential for microbial activity and not necessarily an indication of the community or activity, total microbial DNA analysis is a simple way to begin to investigate correlation among geochemical indicators and microbial processes. To understand the microbial communities that make up the population, functional genes, which encode for specific enzymes such as *nirK* and *nirS* for denitrification and *dsr* for sulfate reduction, were quantified through quantitative PCR (qPCR). This approach identifies microbial populations according to biological functions rather than taxonomy (Throbäck et al., 2004).

3.4.1. Rifle

At the Rifle site, the highest amount of bulk microbial DNA was found in SY02–16 and SY05–16 with 220 ng/g (ng of DNA per g of dry sediment) and 160 ng/g, respectively (Fig. 6, Table A8). However, SY03–18, SY05–18 and SY06–18 also had more than 50 ng/g. The 5–5.5 m (16–18 ft) depth had the highest amount of bulk microbial DNA in all wells where these depths were sampled. Bulk microbial DNA also varied laterally, for example SY01–16 had the lowest bulk microbial DNA with 5 ng/g. Functional genes are reported as a percentage of universal 16S bacteria to quantify what percentage of the bacterial population is capable of denitrification or sulfate reduction. Denitrifying

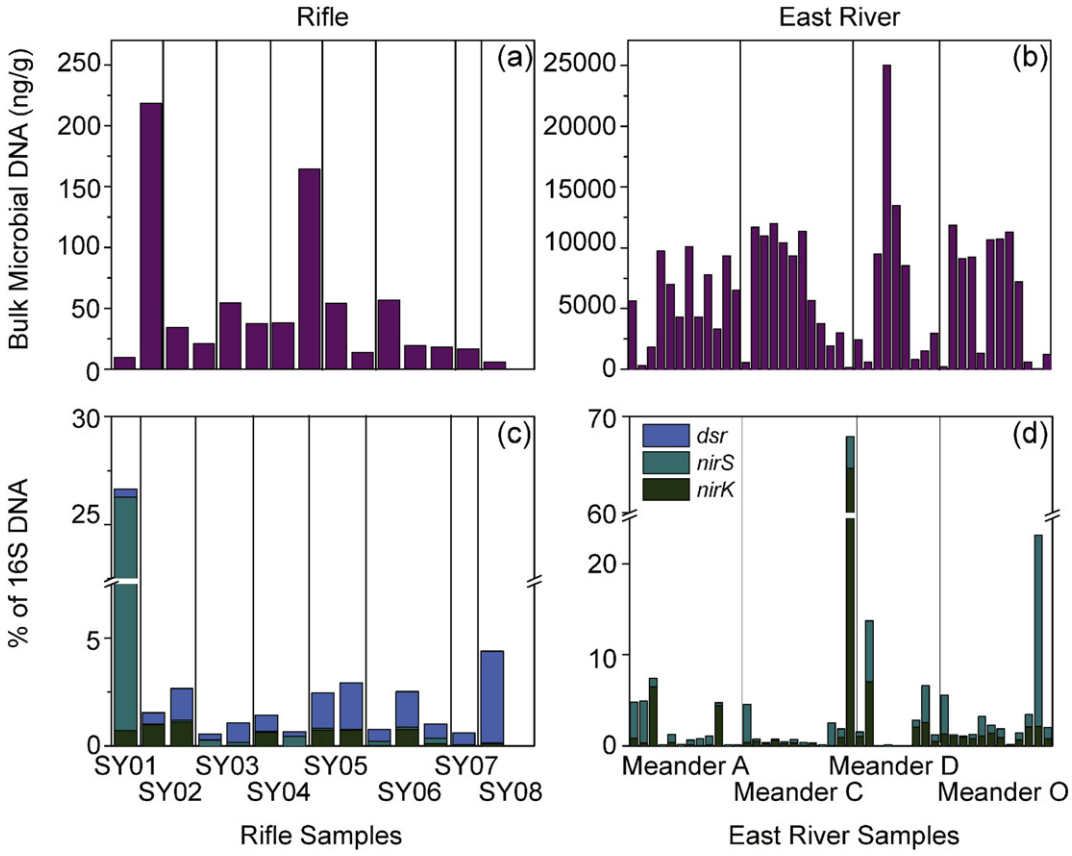


Fig. 6. (a) and (b) Bulk microbial DNA in ng of DNA per g of dry sediment with Rifle in the left column and East River in the right column. (c) and (d) Percentage of bacterial DNA (16S) represented by *nirK* and *nirS* denitrifying bacteria and *dsr* sulfate reducing bacteria. Note the axis breaks on percentage plots. Sulfate reducing bacteria dominated at the Rifle site. Denitrifying bacteria at the East River did not dominate where microbial activity as measured by bulk DNA was highest.

bacteria averaged 0.41% and 0.07% of the bacterial population for *nirK* and *nirS*, respectively, while *dsr* sulfate reducing bacteria averaged 1.1%. Variances in these results were 0.03%, 0.01%, and 0.07%, respectively, excluding the *nirS* result from SY02–16, which had elevated *nirS* percentages of 26% and was the only sample in which denitrifying bacteria was more common than sulfate-reducing bacteria. The abundance of sulfate reducing bacteria at the Rifle site suggests that sulfate reducing conditions exist, as might be expected at sample depths of 3.3 m to 6.7 m with FeS-rich black sediments clearly visible. Sediments closer to the surface may have a stronger denitrifying microbial community.

3.4.2. East River

At the East River, bulk microbial DNA varied from 79 to 25,000 ng/g with an average of 6400 ng/g (Fig. 6, Table A9). Some of these results approached the high and low ends of the detection limit for the instrument. Average concentrations were consistent across meanders with a standard deviation of 730 ng/g among meander averages. The bulk amount of DNA was highest near the center of meanders, which did not correlate to identification of *nir* genes. The percentages of *nir* genes compared to 16S genes were highest near the edges of meanders. As bulk DNA increased (greater than approximately 3000 ng/g), the *nirK* and *nirS* percentages of 16S genes were almost exclusively below 0.01%.

Additional testing of 3 samples (Cc3, Cc5 and Db) with the *dsr* sulfate-reducing gene did not reveal any appropriately amplifying samples. Test samples were chosen because they had more than 15 ng/μl bulk DNA, concentrations high enough that they should amplify if *dsr* genes were present but not so high as to introduce sample-specific inhibition by nucleic acids, humic and fulvic acids or heavy metals (Hargreaves et al., 2013; Schriewer et al., 2011). In addition, test sample Db was a high carbon, high moisture content sample, which would be one of the most likely to have the anaerobic environment ideal for sulfate reducing conditions (Kondo et al., 2004).

At the East River, abundances of *nirK* and *nirS* genes were highest where bulk microbial DNA was lowest, though the continued presence of these genes indicates sustained potential for denitrification. Given the low abundance of nitrogen reducers and undetectable sulfate reduction gene, important terminal electron acceptors at the East River study site are most likely to be those with energetic favorability between denitrification and sulfate reduction, commonly oxidized forms of manganese and iron (Morrice et al., 2000), which is what is often expected in the subsurface (García-Balboa et al., 2011; reviewed by Lovley (1991).

3.5. Multiple linear regression to predict bulk microbial DNA

Because of the heterogeneous nature of soil data, we consider the relationship between the response and predictor to be strong when the adjusted R^2 value is greater than 0.4. The Rifle data acquisition did not include leach tests due to limited sample size; therefore some of the models in Table 1 could not be fit for this data. Models with only extractable metals or only leachable metals for predictors did not perform as well as those including TOC and were eliminated. In addition, leachable

Table 2
Comparison of adjusted R^2 for TOC and TOC-extractable metals models.

Subset of data	Model 1 TOC	Model 4 TOC and extractable Fe and Mn
All East River	0.59	0.69
East River Meanders	0.48	0.65
All East River and Rifle	0.84	0.86
East River Meanders and Rifle	0.85	0.87

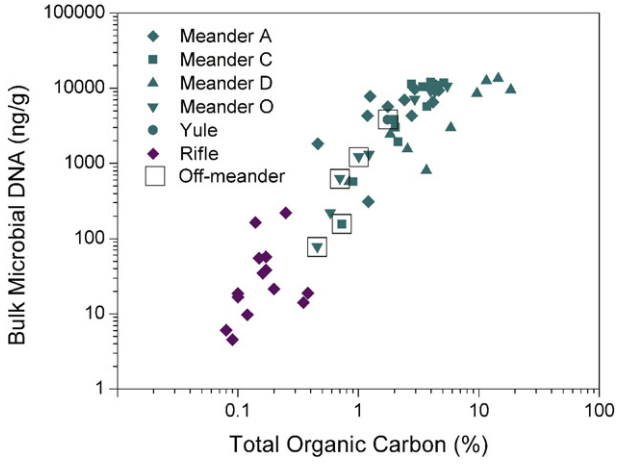


Fig. 7. Bulk microbial DNA as a function of total organic carbon for alluvial Rifle and all East River samples with each meander distinguished by shape.

metals in combination with TOC did not improve the model fit; these models were also removed from consideration. The remaining models presented in Table 2 use the explanatory variables of only TOC or of TOC and extractable iron and manganese (Models 1 and 4 from Table 1). The assumption of homoscedasticity of the residuals was met for all of these models, although Model 1 failed the Shapiro-Wilks test for normality when only East River meander data was included.

Model 1, which was a simple linear regression with TOC only, had a high-adjusted R^2 for all data subsets (Fig. 7). Model 4 that included both TOC and 0.5 N HCl-extractable iron and manganese metals had adjusted R^2 values greater than 0.6 for the East River data and greater than 0.8 for the combination of both datasets. Adding extractable metals consistently resulted in a better model than TOC alone; with the increase in adjusted R^2 between 0.10 and 0.17 for East River data alone but only 0.02 for East River and Rifle data. Therefore, extractable iron and manganese have the potential to be valuable explanatory parameters. Based on these datasets, Model 4 is the best model for estimating bulk microbial DNA because it has the highest R^2, but Model 1 may be more broadly applicable, so the collection of more datasets is needed to confirm both of these models.

For the models fit to the East River data, it was clear that TOC should be included as most adjusted R^2 values are above 0.5. When combining the East River and Rifle datasets, the adjusted R^2 value of both models was always above 0.8. The data subset including the East River meander and Rifle fits Model 4 the best, with the highest R^2 value (0.87), but Model 1 is also a statistically valid model to predict microbial DNA from TOC without extractable Fe and Mn. Additional data from other types of geologic settings should also be collected to investigate whether similar relationships between microbial DNA, TOC and extractable iron and manganese apply to non-floodplain deposits.

4. Conclusions

This study presents data from an investigation of empirical relationships between geochemical parameters and microbial DNA in two floodplain settings. Results of this study suggest that the geochemical properties, TOC and extractable metals, can be used as indicators of areas of inferred high microbial activity in the floodplains studied. The strong relationship between electron donors and bulk microbial DNA has been confirmed in both a stranded floodplain and on active and seasonally active floodplain meanders.

East River soil samples had TOC percentages greater than 1% with a few exceptions along the riverbanks whereas Rifle TOC averaged 0.15%. Average HCl and hydroxylamine hydrochloride extractable iron and manganese were 4700 mg/kg and 150 mg/kg at the East River and 1600 mg/kg and 119 mg/kg at Rifle. Leach tests revealed meander-scale trends in available metals with particularly high iron in meander D. Bulk microbial DNA at Rifle was between 5 and 220 ng/g, much lower than East River samples' average of 6300 ng/g. At Rifle, sulfate reducers are common whereas no evidence of sulfate reducers was found at the East River. In addition, denitrifying bacteria were not highest where bulk microbial DNA was highest, suggesting that iron and manganese may be important electron acceptors across the East River site. The high organic carbon, leachable iron and microbial DNA on meander D may classify this meander as a biogeochemical hotspot with a controlling influence on the nutrient cycling of the system.

Six multiple linear regression models were fit to subsets of the East River and Rifle datasets. The best models to predict patterns of gene expression and/or bulk DNA were determined to consist of TOC alone or TOC, extractable iron and extractable manganese as explanatory variables. Including extractable metals particularly improved fit for data from a single site. The dataset that best fit this model includes samples from within meanders but not from meander bends. More investigation is needed to evaluate whether fluvial processes that influence processes in riverbeds contribute to the empirical relationships observed here. With additional datasets, this model could be used to predict patterns of inferred microbial activity on floodplains based on geochemical indicators alone.

Acknowledgements

This material is based upon work supported as part of the Subsurface Science Scientific Focus Area at Lawrence Berkeley National Laboratory funded by the U.S. Department of Energy, Office of Science, Office of Biological and Environmental Research under Award Number DE-737 AC02-05CH11231. A. Kenwell was supported by the Natural Sciences and Engineering Research Council of Canada (NSERC) and R. Prugue was supported by the Marathon Oil Corporation through student fellowships. We thank four anonymous reviewers whose comments greatly improved the manuscript.

Appendix A. Supplementary data

Supplementary data to this article can be found online at http://dx.doi.org/10.1016/j.scitotenv.2016.04.014.

References

Atchley, A.L., Maxwell, R.M., Navarre-Sitchler, A.K., 2013. Using streamlines to simulate stochastic reactive transport in heterogeneous aquifers: kinetic metal release and transport in CO_2 impacted drinking water aquifers. Adv. Water Resour. 52, 93–106.
Beisman, J., Maxwell, R.M., Navarre-Sitchler, A., Steefel, C., 2015. ParCrunchFlow: an efficient, parallel reactive transport simulation tool for physically and chemically heterogeneous subsurface environments. Comput. Geosci. 19 (2), 403–422.
Boano, F., Harvey, J.W., Marion, A., Packman, A.I., Revelli, R., Ridolfi, L., Wörman, A., 2014. Hyporheic Flow and Transport Processes: Mechanisms, Models, and Biogeochemical Implications. AGU Publications: Reviews of Geophysics, pp. 603–679.
Campbell, K.M., Kukkadapu, R.K., Qafoku, N.P., Peacock, A.D., Lesher, E., Williams, K.H., Bargar, J.R., Wilkins, M.J., Figueroa, L., Ranville, J., Davis, J.A., Long, P.E., 2012. Geochemical, mineralogical and microbiological characteristics of sediment from a naturally reduced zone in a uranium-contaminated aquifer. Appl. Geochem. 27, 1499–1511.
Chapelle, F.H., Lovley, D.R., 1992. Competitive exclusion of sulfate reduction by Fe(III)-reducing bacteria: a mechanism for producing discrete zones of high-iron ground water. Ground Water 30 (1), 29–36.
Chen, D., MacQuarrie, K., 2004. Numerical simulation of organic carbon, nitrate, and nitrogen isotope behavior during denitrification in a riparian zone. J. Hydrol. 293, 235–254.
DOE, 1999. Final Site Observational Work Plan for the UMTRA Project Old Rifle Site, U0042501. DOE, Grand Junction (122 pp.).
DOE, 2011. 2011 Verification Monitoring Report for the Old and New Rifle, Colorado, Processing Sites, S08175. DOE, Grand Junction (118 pp.).
DOE (2), 2011. Review of the Natural Flushing Groundwater Remedy at the Old Rifle Legacy Management Site, Rifle, Colorado, S07263. DOE, Grand Junction (72 pp.).
Du Laing, G., Rinklebe, J., Vandecasteele, B., Meers, E., Tack, F., 2009. Trace metal behavior in estuarine and riverine floodplain soils and sediments: a review. Sci. Total Environ. 407 (13), 3972–3985.
Englert, A., Hubbard, S.S., Williams, K.H., Li, L., Steefel, C.I., 2009. Feedbacks between hydrological heterogeneity and bioremediation induced biogeochemical transformations. Environ. Sci. Technol. 43, 5197–5204.
EPA, 1994. Method 1312: Synthetic Precipitation Leaching Procedure.

Fierer, N., Jackson, J.A., Vilgalys, R., Jackson, R.B., 2005. Assessment of soil microbial community structure by use of taxon-specific quantitative PCR assays. Appl. Environ. Microbiol. 71 (7), 4117–4120.
Fleckenstein, J.H., Krause, S., Hannah, D.M., Boano, F., 2010. Groundwater-surface water interactions: new methods and models to improve understanding of processes and dynamics. Adv. Water Resour. 33 (11), 1291–1295.
García-Balboa, C., Vicente, M.S., Blázquez, M.L., González, F., Muñoz, J.A., Ballester, A., 2011. Iron speciation in dissimilatory Fe(III)-reducing cultures. Geomicrobiol J. 28, 371–379.
Hakala, J.A., Fimmen, R.L., Chin, Y., Agrawal, S.G., Ward, C.P., 2009. Assessment of the geochemical reactivity of Fe-DOM complexes in wetland sediment pore waters using a nitroaromatic probe compound. Geochim. Cosmochim. Acta 73 (5), 1382–1393.
Hargreaves, S.K., Roberto, A.A., Hofmockel, K.S., 2013. Reaction- and sample-specific inhibition affect standardization of qPCR assays of soil bacterial communities. Soil Biol. Biochem. 59, 89–97.
Hedin, L.O., von Fischer, J.C., Ostrom, N.E., Kennedy, B.P., Brown, M.G., Robertson, G.P., 1998. Thermodynamic constraints on nitrogen transformations and other biogeochemical processes at soil-stream interfaces. Ecology 79 (2), 684–703.
Henry, S., Baudoin, E., López-Gutiérrez, J.C., Martin-Laurent, F., Brauman, A., Philippot, L., 2004. Quantification of denitrifying bacteria in soils by nirK gene targeted real-time PCR. J. Microbiol. Methods 59 (3), 327–335.
Hill, A.R., Devito, K.J., Campagnolo, S., Sanmugadas, K., 2000. Subsurface denitrification in a forest riparian zone: interactions between hydrology and supplies of nitrate and organic carbon. Biogeochemistry 51, 193–2000.
Kondo, R., Nedwell, D.B., Purdy, K.J., de Queiroz Silva, S., 2004. Detection and enumeration of sulphate-reducing bacteria in estuarine sediments by competitive PCR. Geomicrobiol J. 21, 145–157.
Li, L., Gawande, N., Kowalsky, M.B., Steefel, C.I., Hubbard, S.S., 2011. Physicochemical heterogeneity controls on uranium bioreduction rates at the field scale. Environ. Sci. Technol. 45, 9959–9966.
Lovley, D.R., 1991. Dissimilatory Fe(III) and Mn (IV) reduction. Microbiol. Rev. 259–287.
McDowell, W.H., Bowden, W.B., Asbury, C.E., 1992. Riparian nitrogen dynamics in two geomorphologically distinct tropical rain forest watersheds: subsurface solute patterns. Biogeochemistry 18, 53–72.
Morrice, J.A., Dahm, C.N., Valett, H.M., Unnikrishna, P.V., Campana, M.E., 2000. Terminal electron accepting processes in the alluvial sediments of a headwater stream. J. N. Am. Benthol. Soc. 19 (4), 593–608.
Murphy, E.M., Ginn, T.R., Chilakapati, A., Resch, C.T., Phillips, J.L., Wietsma, T.W., Spadoni, C.M., 1997. The influence of physical heterogeneity on microbial degradation and distribution in porous media. Water Resour. Res. 33 (5), 1087–1103.
Pepe-Ranney, C., Berelson, W.M., Corsetti, F.A., Treants, M., Spear, J.R., 2012. Cyanobacterial construction of hot spring siliceous stromatolites in Yellowstone National Park. Environ. Microbiol. 14 (5), 1182–1197.
Pinay, G., Black, V.J., Planty-Tabacchi, A.M., Gumiero, B., Décamps, H., 2000. Geomorphic control of denitrification in large river floodplain soils. Biogeochemistry 50, 163–182.
Pinay, G., Gumiero, B., Tabacchi, E., Gimenez, O., Tabacchi-Planty, A.M., Hefting, M.M., Burt, T.P., Black, V.A., Nilsson, C., Iordache, V., Bureau, F., Vought, L., Petts, G.E., Décamps, H., 2007. Patterns of denitrification rates in European alluvial soils under various hydrological regimes. Freshw. Biol. 52, 252–266.
Prommer, H., Tuxen, N., Bjerg, P.L., 2006. Fringe-controlled natural attenuation of phenoxy acids in a landfill plume: integration of field-scale processes by reactive transport modeling. Environ. Sci. Technol. 40, 4732–4738.
Revelli, R., Boano, F., Camporeale, C., Ridolfi, L., 2008. Intra-meander hyporheic flow in alluvial rivers. Water Resour. Res. 44, W12428.
Schilling, K.E., Jacobson, P., 2012. Spatial relations of topography, lithology and water quality in a large river floodplain. River Res. Appl. 28, 1417–1427.
Schriewer, A., Wehlmann, A., Wuertz, S., 2011. Improving qPCR efficiency in environmental samples by selective removal of humic acids with DAX-8. J. Microbiol. Methods 85, 16–21.
Sena, C., Molinero, J., Ajima, S., Todaka, N., 2012. Modelling microbial degradation coupled to reactive transport in groundwater: a benchmark analysis. Math. Geosci. 44, 209–226.
Sheather, S., 2009. A Modern Approach to Regression With R. Springer, New York: NY.
Staroscik, A., 2004. Calculator for Determining the Number of Copies of a Template. URI Genomics & Sequencing Center (<http://cels.uri.edu/gsc/cndna.html>).
Sweerts, J.R., Bär-Gilissen, M., Cornelese, A.A., Cappenberg, T.E., 1991. Oxygen-consuming processes at the profundal and littoral sediment-water interface of a small meso-eutrophic lake (Lake Vechten, The Netherlands). Limnol. Oceanogr. 36 (6), 1124–1133.
Throbäck, I.N., Enwall, K., Jarvis, A.S., Hallin, S., 2004. Reassessing PCR primers targeting nirS, nirK and nosZ genes for community surveys of denitrifying bacteria with DGGE. FEMS Microbiol. Ecol. 49, 401–417.
Yabusaki, S.B., Fang, Y., Williams, K.H., Murray, C.J., Ward, A.L., Dayvault, R.D., Waichler, S.R., Newcomer, D.R., Spane, F.A., Long, P.E., 2011. Variably saturated flow and multicomponent biogeochemical reactive transport modeling of a uranium bioremediation field experiment. J. Contam. Hydrol. 126, 271–290.